International Journal of Minerals, Metallurgy and Materials
Volume 22, Number 12, December 2015, Page 1328
DOI: 10.1007/s12613-015-1201-0

Plasma preparation and low-temperature sintering of spherical TiC–Fe composite powder

Jian-jun Wang[1,2], *Jun-jie Hao*[1], *Zhi-meng Guo*[1], *and Song Wang*[1]

1) Institute for Advanced Materials and Technology, University of Science and Technology Beijing, Beijing 100083, China
2) Research and Development Center, CSR Qingdao Sifang Co., Ltd., Qingdao 266111, China
(Received: 31 March 2015; revised: 19 July 2015; accepted: 21 July 2015)

Abstract: A spherical Fe matrix composite powder containing a high volume fraction (82vol%) of fine TiC reinforcement was produced using a novel process combining *in situ* synthesis and plasma techniques. The composite powder exhibited good sphericity and a dense structure, and the fine sub-micron TiC particles were homogeneously distributed in the α-Fe matrix. A TiC–Fe cermet was prepared from the as-prepared spherical composite powder using powder metallurgy at a low sintering temperature; the product exhibited a hardness of HRA 88.5 and a flexural strength of 1360 MPa. The grain size of the fine-grained TiC and special surface structure of the spherical powder played the key roles in the fabrication process.

Keywords: powder technology; cermets; radio frequency plasma; sintering; numerical simulation

1. Introduction

As a typical metal matrix composite (MMC), TiC–Fe cermet draws significant attention because of its extremely high hardness and toughness. This unique combination of mechanical properties makes TiC–Fe very attractive for manufacturing high-performance wear parts and cutting tools [1–4]. In general, two routes are used to add reinforcement to the Fe matrix: direct addition and *in situ* synthesis [5–10]. These broad categories can be further divided into more specialized processes such as powder metallurgy (PM), self-propagating high-temperature synthesis (SHS), and reaction casting [11–12]. TiC–Fe composites are currently produced by PM routes involving the addition of TiC powder to Fe powder. The PM technique allows the use of a higher volume fraction of the ceramic particles but generally suffers from contaminated matrix–reinforcement interfaces and low wettability. One way to overcome these issues is to synthesize the TiC particles *in situ*. *In situ* synthesis techniques such as SHS and reaction casting involve a chemical reaction, resulting in the formation of a fine and thermodynamically stable ceramic phase within the metal matrix. Although effective, the SHS technology imposes limitations on the intrinsic porosity during the reaction. Moreover, manufacturing the TiC–Fe composites using casting encounters certain difficulties. There are problems associated with accommodating the volume fraction and attaining an even distribution of the TiC reinforcement because of the density difference between Fe and TiC and reduction of the liquid steel fluidity at high TiC levels. Thus, the higher volume fraction of the TiC reinforcement conflicts with the even distribution and wettability achieved using the current methods.

Radio frequency (RF) plasma technology is especially useful for spheroidizing and synthesizing powder materials because of the relatively long available residence time and high quenching rate, which increase the number of nuclei and strongly suppress the growth of the product powders [13–14]. Hence, a novel process is described in this study, where *in situ* techniques with plasma processing were used to manufacture spherical TiC–Fe composite powders with a high level of fine-sized TiC. Low-temperature sintering was used to prepare the TiC–Fe cermet. This article focuses on the reaction path, microstructure, and properties of the product.

Corresponding author: Jun-jie Hao E-mail: haojunjie@ustb.edu.cn

2. Experimental

In this experiment, the feedstock powder was prepared with a Ti:C molar ratio of 1:1. To obtain highly reactive and high-purity amorphous C, sucrose was used in the experiment. Ferrotitanium (FeTi70) powder and sucrose were mixed in the presence of absolute ethyl alcohol as the dispersing agent for approximately 12 h using a planetary ball mill. Then, the ball milling mixture was pyrolyzed for 2 h at 250°C and for 1 h at 350°C in a flowing Ar atmosphere, under which sucrose was completely carbonized. Finally, the Ti–Fe–C system feedstock powder was prepared by crushing and sieving the carbonized aggregates.

The experimental apparatus (as shown in Fig. 1) consisted of an RF inductively coupled plasma torch (3.5 MHz, 100 kW), water-cooled steel chamber, powder feeder, and vacuum system (as high as 1.0×10^{-3} Pa). In this experiment, a stable plasma was first generated using Ar as the center gas and a sheath gas with flow rates of 28 $L \cdot min^{-1}$ and 85 $L \cdot min^{-1}$, respectively. The feedstock powders were axially injected into the plasma torch at an Ar carrier flow rate of 5 $L \cdot min^{-1}$, and then, spherical powders were collected at the bottom of the heat-exchange chamber. The experimental parameters used for the RF plasma processing of the TiC–Fe powders are listed in Table 1. The as-prepared TiC–Fe powders were compacted (350 MPa), vacuum sintered (1200°C for 2 h), and hot treated (oil quenched at 900°C and low-temperature tempered at 200°C for 2 h) in sequence to obtain bulk TiC–Fe composites. Scanning electron microscopy (SEM) and X-ray diffraction (XRD) were used to characterize the morphology and phase composition of the specimen before and after plasma processing. The hardness and flexural strength of the sintered samples were tested using a Rockwell hardness tester and universal testing machine.

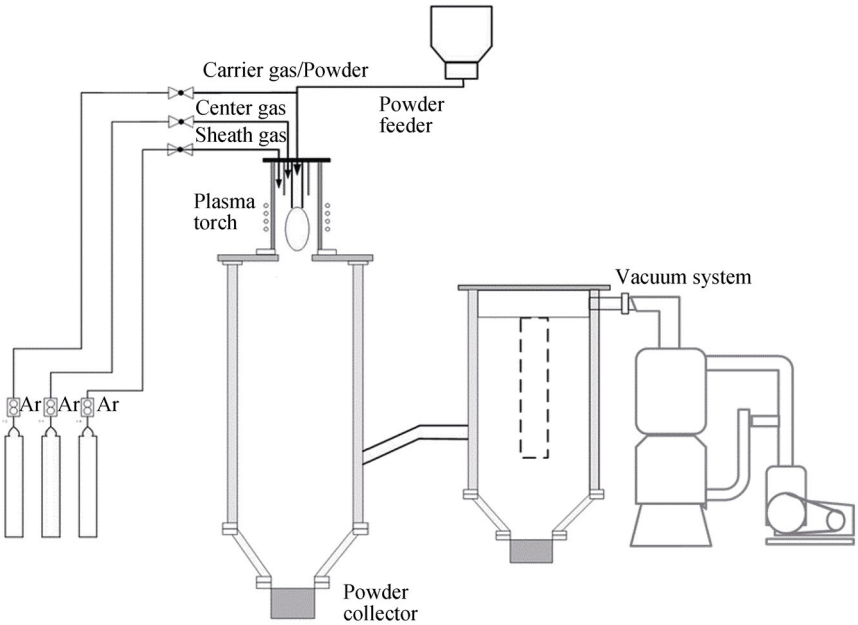

Fig. 1. Schematic illustration of the plasma processing equipment.

Table 1. Experimental parameters for RF plasma processing

Carrier gas flow rate (argon), Q_1 / ($L \cdot min^{-1}$)	5
Center gas flow rate (argon), Q_2 / ($L \cdot min^{-1}$)	28
Sheath gas flow rate (argon), Q_3 / ($L \cdot min^{-1}$)	85
Powder feed rate / ($g \cdot min^{-1}$)	10
Reactor pressure / KPa	90
Plasma power / kW	65

To evaluate the synthesis process, a two-dimensional finite element model was computed and analyzed using FLUENT software. GAMBIT software was employed for geometric modeling and meshing based on the characteristic dimensions of the plasma generator, as illustrated in Fig. 2. The mathematical model included Maxwell and conservation equations for the RF plasma. The plasma model was based on assumptions that the plasma was a steady-state turbulent flow in an axisymmetric cylindrical geometry, in local thermodynamic equilibrium, and optically thin, and that there was negligible viscous dissipation. Therefore, the flow field of the plasma reactor was computed using the standard κ–ε turbulent model and PISO pressure–velocity coupling algorithm with a pressure relaxation factor of 0.3 and a speed relaxation factor of 0.7.

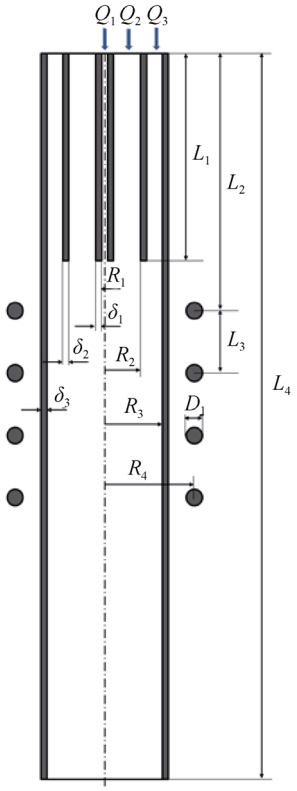

Fig. 2. Characteristic dimensions of the plasma reactor: L_1 = 100 mm, L_2 = 120 mm, L_3 = 30 mm, L_4 = 350 mm, R_1 = 1.5 mm, R_2 = 18 mm, R_3 = 29 mm, R_4 = 45 mm, $\delta_1 = \delta_2 = \delta_3$ = 3 mm, and D_1 = 8 mm.

3. Results and discussion

Fig. 3(a) shows the raw morphology of the Ti–Fe–C feedstock powder. The feedstock powder is irregular, ranging in size from 45 to 75 μm. Fig. 3(b) presents an SEM micrograph of the plasma-prepared powder. The majority of the products exhibit good spherical shapes, which indicates that the Ti–Fe–C feedstock powder can be melted and spheroidized with the combination of a plasma flame and the heat of the *in situ* reaction. However, more or less imperfect spheroidization occurs, which can be improved by the appropriate adjustment of the plasma processing parameters.

Fig. 3(c) presents an XRD diffraction pattern of the spherical composite powder, in which the detectable phases are TiC and α-Fe. According to the thermodynamics analysis [15–16], the standard Gibbs free energy of the TiC formation is lower, compared with Fe_2Ti and Fe_3C. Hence, the formation of the TiC phase is favored over Fe_2Ti and Fe_3C. Because of the very short plasma processing time, there is not sufficient time for the other phases to form.

Fig. 4 presents cross-sectional SEM images of the microstructures of the feedstock powder and spherical TiC–Fe powder. The feedstock powder is composed of ferrotitanium particles with sizes of less than 5 μm and amorphous C, which acts as a binder between the ferrotitanium powder

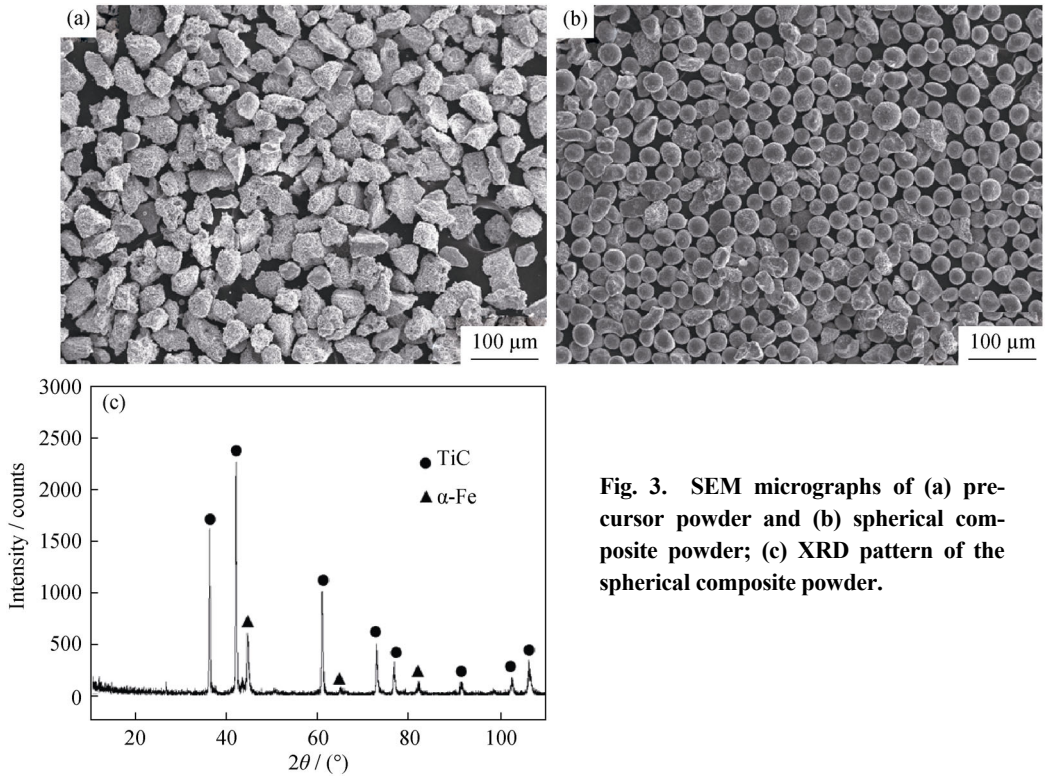

Fig. 3. SEM micrographs of (a) precursor powder and (b) spherical composite powder; (c) XRD pattern of the spherical composite powder.

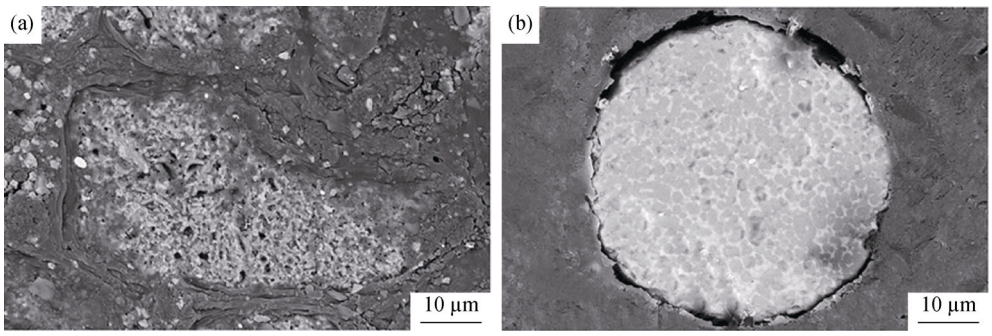

Fig. 4. Cross-sectional SEM micrographs of powder before and after plasma processing: (a) precursor powder; (b) spherical composite powder.

particles. A comparison of the cross-sectional SEM micrograph (Fig. 4(b)) with the XRD pattern of the spherical TiC–Fe composite powder indicates that the gray phase is TiC and the white phase is the Fe matrix. The TiC grains are spherically shaped, uniformly distributed, and have uncontaminated surfaces in the Fe matrix. There is good wettability between the binder matrix and TiC reinforcement; hence, a strong bonding interface can be obtained. Furthermore, the volume fraction of the TiC fabricated by the novel process can reach 82vol%, while the average diameter of the TiC grains can remain at approximately 1 μm, which has been impossible to achieve using other methods. To obtain TiC particles with sizes of 1 μm using conventional methods, the content of liquid Fe must usually be greater than 50% [17–18]. However, using this approach, the TiC–Fe composite powder with uniform dispersion of a high volume fraction of fine TiC grains can be achieved under a combination of a high enough energy, short processing time, and fast cooling rate, even though the Fe content is low.

Fig. 5 presents the numerical results for the temperature field of the plasma reactor. The plasma torch has a heart-shaped high-temperature region with a maximum value of 10148 K, which can provide enough energy for melting, synthesis, and spheroidization. Therefore, the melting–solution–precipitation mechanism can be used to explain the synthesis of TiC–Fe. As illustrated in Fig. 6, initially, the surface of the original aggregate (Fig. 6(a)) absorbed heat from the plasma torch and then melted. The Fe–Ti liquid formed first (Fig. 6(b)); hence, the wetting of the powder particles increased. As the temperature increased, the dissolution of the amorphous C particles and then the formation and precipitation of TiC were accelerated. At the same time, the liquid phase was promoted by the high-temperature plasma from the exterior to the interior. As a result, whole molten droplets can be produced (Fig. 6(c)). In the molten droplets, however, there was no crystal nucleus of heterogeneous nucleation, and supersaturation over the equilibrium concentration occurred. Thus, the nucleation mode of the round fine TiC particles is homogeneous nucleation. The small size of the TiC grains is attributed to the rapid melting and cooling, depending on the RF plasma generator. Finally, the surface tension transformed the droplets into spherical solid particles with a high level of fine TiC reinforcement (Fig. 6(d)).

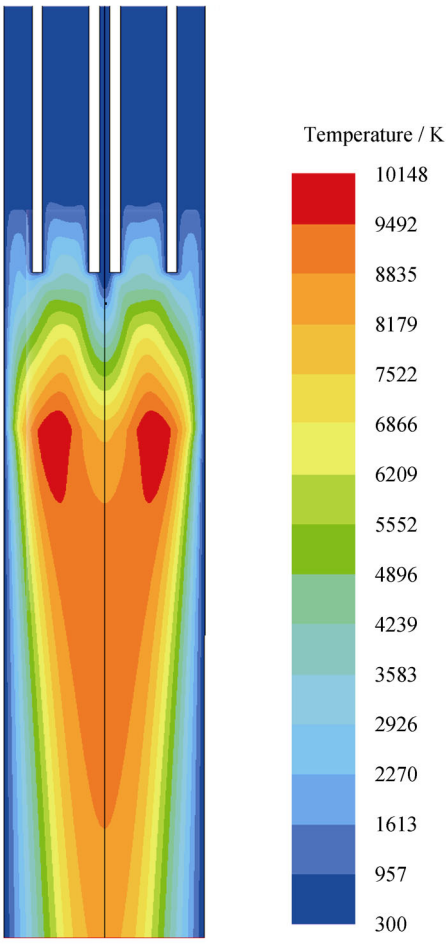

Fig. 5. Temperature field of the plasma reactor.

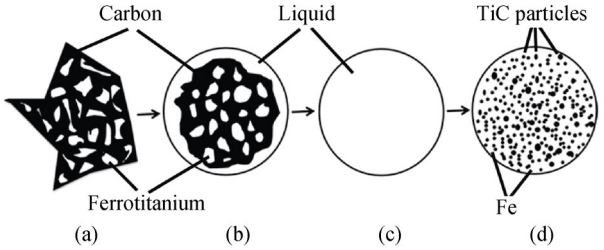

Fig. 6. Schematic illustration of the reaction mechanism: (a) original aggregate; (b) Fe–Ti liquid formed; (c) whole molten droplets; (d) spherical solid particles with a high level of fine TiC reinforcement.

Fig. 7(a) presents an SEM image of the microstructure of the TiC–Fe composite. The TiC–Fe cermet with fine TiC grains is compact, uniform, and free from cracks. The low sintering temperature can prevent TiC grain growth. Fig. 7(b) shows the special surface morphology of the composite powder. The outer layers of the powder consisted of Fe; thus, the sintering process was actually equivalent to the sintering of Fe layers of the adjacent particles (Fig. 7(c)), which can be completed at 1200°C. Furthermore, during the powder compacting and sintering processing, the cohesive powder strength was improved by the "gear bite", which depends on the uneven surface of the spherical powder. The hardness of HRA 88.5 and flexural strength of 1360 MPa were achieved by heat treatment of the composites. This novel method is less expensive and more efficient than other methods.

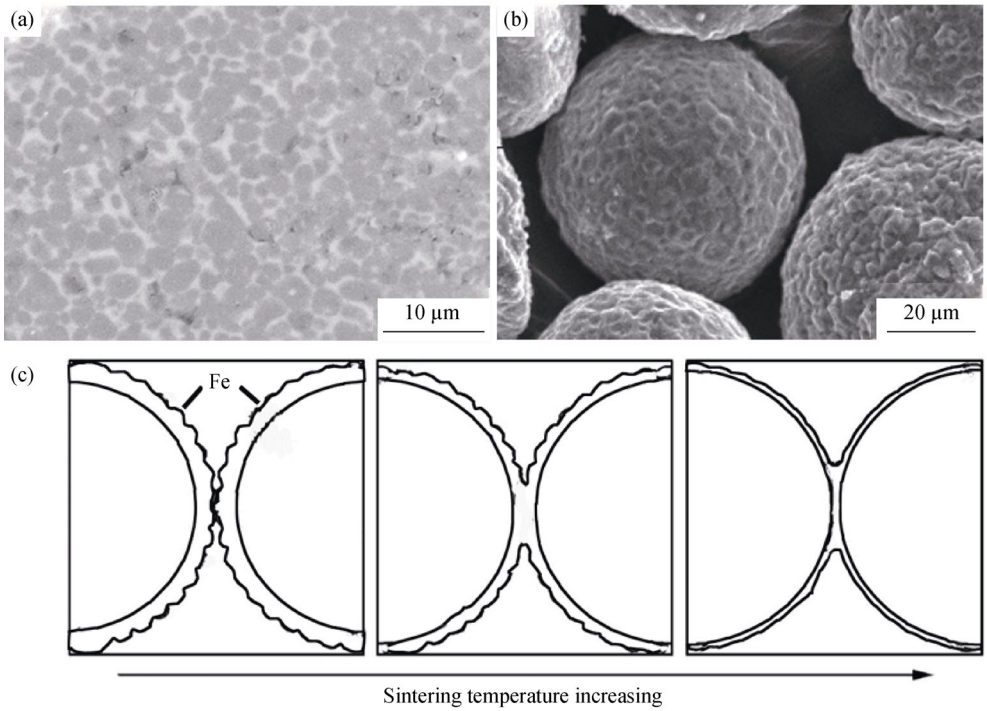

Fig. 7. (a) SEM micrographs of the sintered sample; (b) surface morphology of the spherical composite powder; (c) schematic diagram of the TiC–Fe composite particle sintering process.

4. Conclusions

(1) In summary, using a novel process combining an *in situ* reaction with plasma techniques, a spherical TiC–Fe composite powder was successfully produced. The main innovation of this technique is that the volume fraction of TiC is approximately 82vol%, while the average diameter of the TiC grains can remain at approximately 1 μm. The adequate high energy, short processing time, and fast cooling rate of the plasma torch play the key roles in the melting–solution–precipitation process. The TiC grains formed by the special *in situ* reaction are fine, spherical, and uniformly dispersed and have a clean interface with the metal matrix.

(2) The TiC–Fe cermet sintered at low temperature exhibited high hardness and flexural strength because of the fine TiC grain size and special surface structure of the powder.

(3) The spherical composite powder was also appropriate for hot spraying and other PM techniques. Used as a material for injection molding, it is expected to boost the near net shape technology of the TiC–Fe cermet. Different grades of the TiC–Fe cermet powder can be prepared by adjusting the

process parameters. The method described in this study is also applicable to other MMC systems.

Acknowledgements

This work was financially supported by the National Natural Science Foundation of China (No. 51274039) and the Research Fund for the Doctoral Program of Higher Education of China (No. 20120006110007).

References

[1] H.C. Man, S. Zhang, F.T. Cheng, and T.M. Yue, *In situ* synthesis of TiC reinforced surface MMC on Al6061 by laser surface alloying, *Scripta Mater.*, 46(2002), No. 3, p. 229.

[2] S.F. Wei, K.Q. Feng, H.S. Chen, J. Xiong, H.Y. Fan, G.M. Zhang, and H. Wang, Combustion synthesis of TiC/Fe–Cu composites under an electric field, *J. Alloys Compd.*, 541(2012), p. 186.

[3] H. Zhang, Y. Zou, Z.D. Zou, and C.W. Shi, Effects of chromium addition on microstructure and properties of TiC–VC reinforced Fe-based laser cladding coatings, *J. Alloys Compd.*, 614(2014), p. 107.

[4] S. Corujeira Gallo, N. Alam, and R. O'Donnell, *In-situ* synthesis of titanium carbides in iron alloys using plasma transferred arc welding, *Surf. Coat. Technol.*, 225(2013), p. 79.

[5] S.C. Tjong and Z.Y. Ma, Microstructural and mechanical characteristics of in situ metal matrix composites, *Mater. Sci. Eng. R*, 29(2000), No. 3-4, p. 49.

[6] K. Das, T.K. Bandyopadhyay, and S. Das, A review on the various synthesis routes of TiC reinforced ferrous based composites, *J. Mater. Sci.*, 37(2002), No. 18, p. 3881.

[7] L.S. Zhong, Y.H. Xu, M. Hojamberdiev, J.B. Wang, and J. Wang, *In situ* fabrication of titanium carbide particulates-reinforced iron matrix composites, *Mater. Des.*, 32(2011), No. 7, p. 3790.

[8] K. Das and T.K. Bandyopadhyay, Effect of form of carbon on the microstructure of in situ synthesized TiC-reinforced iron-based composite, *Mater. Lett.*, 58(2004), No. 12-13, p. 1877.

[9] J. Wang and Y.S. Wang, In-situ production of Fe–TiC composite, *Mater. Lett.*, 61(2007), No. 22, p. 4393.

[10] M. Razavi, M.S. Yaghmaee, M.R. Rahimipour, and S.S. Razavi-Tousi, The effect of production method on properties of Fe–TiC composite, *Int. J. Miner. Process.*, 94(2010), No. 3-4, p. 97.

[11] K.Q. Feng, Y. Yang, B.L. Shen, and L.B. Guo, *In situ* synthesis of TiC/Fe composites by reaction casting, *Mater. Des.*, 26(2005), No. 1, p. 37.

[12] P. Persson, A.E.W. Jarfors, and S. Savage, Self-propagating high-temperature synthesis and liquid-phase sintering of TiC/Fe composites, *J. Mater. Process. Technol.*, 127(2002), No. 2, p. 131.

[13] P. Rai, J.S. Park, G.G. Park, W.M. Lee, Y.T. Yu, S.K. Kang, S.Y. Moon, and B.G. Hong, Influence of carbon precursors on thermal plasma assisted synthesis of SiC nanoparticles, *Adv. Powder Technol.*, 25(2014), No. 2, p. 640.

[14] S. Choi, L.D.S. Lapitan Jr, Y.Y. Cheng, and T. Watanabe, Synthesis of cobalt boride nanoparticles using RF thermal plasma, *Adv. Powder Technol.*, 25(2014), No. 1, p. 365.

[15] H.G. Zhu, K. Dong, H. Wang, J.W. Huang, J.L. Li, and Z.H. Xie, Reaction mechanisms of the TiC/Fe composite fabricated by exothermic dispersion from Fe–Ti–C element system, *Powder Technol.*, 246(2013), p. 456.

[16] I. Barin, O. Kubaschewski, and O. Knacke, *Thermochemical Properties of Inorganic Substances: Supplement*. Springer, 2014.

[17] R. Licheri, R. Orrù, G. Cao, A. Crippa, and R. Scholz, Self-propagating combustion synthesis and plasma spraying deposition of TiC–Fe powders, *Ceram. Int.*, 29(2003), No. 5, p. 519.

[18] Y. Choi and S.W. Rhee, Effect of iron and cobalt addition on TiC combustion synthesis, *J. Mater. Res.*, 8(1993), No. 12, p. 3202.